Aerating Fuel Nozzle Design Influences on Airflow Features

T. J. Rosfjord*
United Technologies Research Center, East Hartford, Connecticut 06108
and
W. A. Eckerle†
Cummins Engine Company, Columbus, Indiana 47202

The velocity and turbulence levels downstream of eight variations of a model gas turbine, aerating, fuel nozzle have been measured. The nozzle configurations were assemblies that purposefully altered the airflow through the nozzle by misaligning swirlers, changing the number of vanes in a swirler, or contouring swirl vane trailing edges. Data were acquired by a traversing, two-component laser velocimeter in planes 0.060 in. (1.5 mm) or 2.50 in. (6.4 cm) downstream from the nozzle exit. Analyses of these data indicated that very symmetric flowfields can be produced. Such control was easier to achieve for the airflow than the fuel, supporting the position that nozzle patternation quality was more dependent on the fuel distribution in the nozzle. The presence of swirler wakes could always be discerned at the nozzle exit; the extreme variations imposed by coarse swirlers could dominate the flow. Such airflow influences were not apparent in the velocity profiles at downstream locations. However, their influence in convecting a higher fuel mass flux persisted from the nozzle exit and produced extreme variations in the spray pattern.

Introduction

MOST modern gas turbine combustor systems use an aerating fuel nozzle. In such a device, the fuel is injected as a thin annular sheet with high velocity airflows adjacent to both the inner and outer surfaces of the sheet. Unlike a pressure-atomizing nozzle, the aerating nozzle (sometimes referred to as an airblast nozzle) does not rely upon achieving a high fuel velocity, as produced by a high fuel path pressure loss, to atomize and distribute the liquid. Rather these responsibilities are assigned to the airflows, which shear the fuel film and carry the droplets along the airflow trajectory. The airflows are driven by the pressure drop established by the combustor liner; for a nominal 3% loss liner, airflow velocities in excess of 350 ft/s (107 m/s) would be produced at a high power condition. Because the aerating nozzle performance principally depends on the airflow and not the fuel flow, it has demonstrated the ability to achieve high levels of atomization for wide ranges of fuel flow rate and with relative insensitivity to the properties of the fuel. Both of these features represent distinct advantages over the pressure-atomizing nozzle. In contrast, the aerating nozzle promotes a coupling between the air and fuel flow rates that can be disadvantageous. For example, atomization and distribution are harder to achieve at lightoff conditions for which the airflow momentum is very low. Also, the fuel and air coupling could result in undesirable heat release profiles for transient operation. Since the nozzle uses a delicate balance of air and fuel momenta to achieve atomization and distribution characteristics, it also displays a greater sensitivity to improper design and manufacturing practices; nonsymmetric sprays can easily result. The consequent fuel-air mixtures could produce heat loads that damage the combustor or turbine or produce unacceptable levels of gaseous and particulate emissions.

Other investigators have characterized the flowfield downstream of a swirler. For example, Kilik[1-3] has mapped the flows produced by an isolated axial flow, high swirl strength annular swirler using five-hole pressure probing and hot-wire anemometry. In his several studies, he has discerned the influence of swirler design features such as vane shape, angle, aspect ratio, spacing, and overall blockage ratio on the mean and turublent flowfield, particularly in the vicinity of the midstream recirculation zone. Sander and Lilley[4] and Lilley[5] have also studied flowfields produced by annular vane swirlers for the purpose of defining the initial conditions for combustor computational fluid dynamic calculations. Gas turbine engine fuel nozzle manufacturers have studied the flows produced by swirlers since, as stated above, the swirling airflow through modern aerating nozzles is primarily responsible for the fuel atomization and distribution. Two reported studies[6,7] were aimed at the gross features of the flow produced by an isolated swirler, particularly the effective flow area and swirl number. All of these investigations studied isolated swirlers. That is, they documented the flow features and details of an axial flow, annular vane swirler that was not packaged in an aerating fuel nozzle. The latter instance differs in that usually multiple swirling flows are present, with the nozzle design purposefully attempting to cause them to interact. One study has been reported that attempted to interpret the lean stability characteristics of a single fuel nozzle test combustor in terms of the flowfields produced by its aerating fuel nozzle.[8] Results showed a relationship between certain aerating nozzle features (e.g., split of airflow to each of two swirl paths) to the lean blowout limit of the combustor.

The study reported in this manuscript differs from previous studies by detailing the flow produced by an aerating nozzle containing two interacting swirl flows and using the results to interpret previously obtained fuel spray patternation data. A previous United Technologies Research Center (UTRC) study[9] documented the influences of design and manufacturing practices on the circumferential uniformity of the spray formed by an aerating nozzle. Detailed liquid patternation data were acquired for 33 nozzle configurations including nine which purposely imposed alterations on the nozzle airflow patterns. This manuscript reports the results of a complementary study that focused on measuring the airflow velocities for eight of those airflow configurations. Data were acquired for the three velocity components, the normal turbulent stresses, and, for some cases, the correlated Reynolds stress in planes 0.060 in. (1.5 mm) and 2.50 in. (6.4 cm) downstream from the nozzle exit. The data were analyzed to discern the sensitivity of

Presented as Paper 88-3140 at the AIAA/ASME/SAE/ASEE 24th Joint Propulsion Conference, Boston, MA, July 11-13, 1988; received June 6, 1989; revision received March 7, 1990.

*Senior Project Engineer, Power and Industrial Systems Technology. Associate Fellow AIAA.
†Fluids Metrologist. Member AIAA.

the air flowfield structure to nozzle design variations. When coupled with results from the previous study, conclusions could be drawn concerning airflow influences on spray patternation. The data could also be used to evaluate the effectiveness of computational fluid dynamics codes to predict the development of multidimensional, swirling flowstreams.

Test Program

The model nozzle used in this study (Fig. 1) was the same device used in the previously cited spray study. It was sized as a nominally 850 lb/h (390 kg/h) fuel flow device, which delivered inner and outer clockwise swirled airstreams on either side of the fuel annulus. In this airflow study, fuel was not delivered to the nozzle. The outer airflow was swirled by an annular, axial flow swirler with flowpath inner diameter (ID), outer diameter (OD), and length of 0.90, 1.34, and 0.34 in. (2.28, 3.40, and 0.86 cm), respectively. The swirler contained curved vanes with a final turning angle of 50 deg. The baseline nozzle assembly contained a 14-vane outer swirler. The inner swirler contained 50-deg, straight vanes in a 0.44-in. (1.1-cm) diam circular core air pipe. Six vanes were in the baseline core swirler. The endcap imparted a radial inflow component to the nozzle stream prior to discharging through a 0.91-in. (2.3-cm) diam orifice; a velocity vector normal to the minimum flow area formed a 60-deg angle with the nozzle axis.

As stated, fuel was not delivered to the nozzle during the airflow measurements; laser velocimeter (LV) signals from spray droplets would not represent the airflow. In a subsequent study, the fuel and air flowfields produced by a model aerating nozzle very similar to the device used in the current study were interrogated by both LV and phase-Doppler diagnostics.[10] The latter instrument was used to track both the total liquid phase and, by extrapolation from the smallest droplets, the gas-phase in the presence of the liquid. The LV was again used with airflow only. The gas-phase axial velocity data tracked the LV data well at axial stations from 1 in. (2.54 cm) to 2 in. (5.08 cm) downstream of the nozzle. The measured axial turbulence levels were lower in the presence of the spray. However, this judgment was based on tracking droplets with diameters two to four times larger than the LV titanium dioxide seed and therefore may overstate the damping influence of the spray. The concurrence of the LV airflow data and phase-Doppler gas-phase data indicated that measurements reported for the current program would be representative of an operating aerating nozzle.

The focus of this effort was to measure and interpret air velocity and turbulence levels for model nozzle configurations that imposed variations on the nozzle airflow. The alterations emphasized the following three features (baseline and altered components are indicated):

1) Airflow alignment:
   Baseline: Perfectly axially aligned.
   Variation: Endcap and outer swirler were canted 2.5 deg from the nozzle axis.

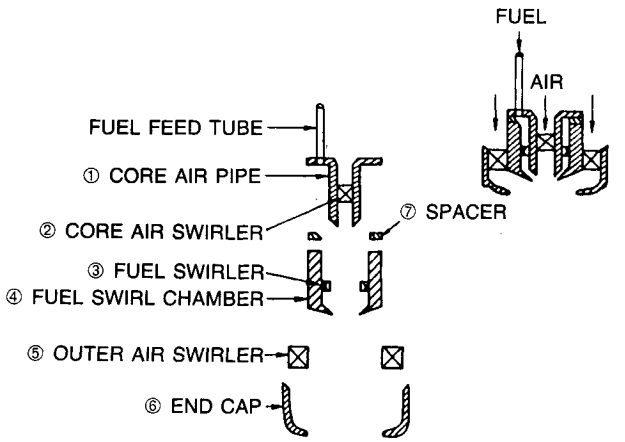

Fig. 1 Model aerating nozzle.

2) Number of swirler vanes:
   Baseline: Inner—6 vanes; outer—14 vanes.
   Variation: a) 3-vane inner swirler achieved by removing alternate blades; b) 7-vane outer swirler achieved by removing alternate blades; and c) tandem combinations of six vane swirlers.
3) Outer swirler trailing edge shape:
   Baseline: Rounded trailing edge.
   Variation: a) Square and b) knife-edge shape.

A detailed discussion of the role of each of these alterations on fuel circumferential uniformity can be found in Ref. 9. In general, it was concluded that the fuel exit annulus was a critical feature in achieving symmetric spray patterns. Airflow influences had a generally lesser impact on fuel patternation, although severe nonuniformities can be imposed by poorly designed airflow management components. Figure 2 presents an example of the fuel distortion that resulted from an imperfect airflow. Depicted are contour plots of fuel flux determined 2.5 in. (6.4 cm) downstream from the baseline configuration (Fig. 2a) and for one in which the outer endcap was misaligned by 2.5 deg from the nozzle axis (Fig. 2b). For the latter case, the pattern is shifted off-axis by an amount greater than 2.5 deg.

The test apparatus used in this study consisted of a conventional air supply system, a laser velocimeter system, and a precision positioning system. All of the tests were conducted in the UTRC Jet Burner Test Stand with the airflow discharging into the atmosphere. The nozzle airflow pressure drop was held constant at 7-in. H_2O. This level, set to assure that seed particles were not centrifuged from the inner regions of the flowfield, corresponds to a nominally 2% loss liner. Measurements included axial, radial, and tangential velocities and normal turbulent stresses; in some cases correlated axial-radial and axial-tangential Reynolds stress were also obtained. These measurements were performed along 5-deg increment circumferential traverses at typically nine radial positions. Such measurements were performed in a plane 0.060 in. (1.5 mm) downstream of the nozzle for every configuration; they were also obtained in a plane 2.5 in. (6.4 cm) downstream for limited configurations. Table 1 indicates the type and location

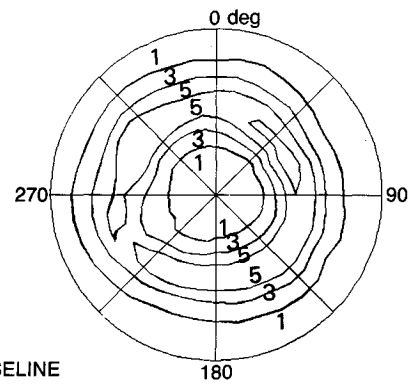

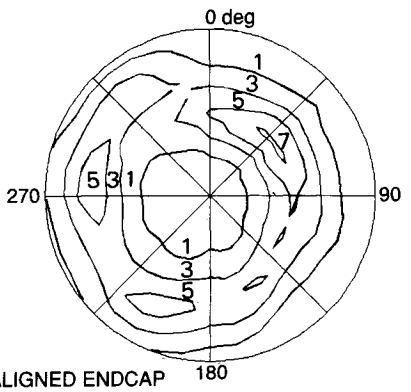

Fig. 2 Misaligned airflow distorted the fuel spray.

of data acquired for the eight configurations; the identification number is the one retained from the original liquid patternation study.

The velocity measurements were made using a TSI Model 9100-7, two-channel velocimeter. A 2-W argon-ion laser was used with frequency shifting by Bragg cells in both the blue and green beams to permit resolution of negative velocities. The seed material was titanium dioxide having a characteristic size less than 1 μ. Seed rates were adjusted to achieve processor count rates of 100–300 Hz. In order to perform the measurements as close to the nozzle face as possible, a small beam convergence angle (1.67 deg) for the rays in the plane normal to the injector face (i.e., axial velocity) was used, producing an elongated probe volume. As a consequence, off-axis collection optics were required to achieve the desired spatial resolution. A forward-scatter, 30-deg off-axis system was used with the collection optics mounted rigidly to the velocimeter platform.

A flange on the endcap was used to mount the nozzle on the end plate of a cylindrical plenum. This assembly was mounted on a stepper-motor-driven rotary table (0.02 deg/step resolution) in a manner to precisely align the nozzle axis with the axis of revolution. The velocimeter was always oriented with the blue beams producing fringe patterns normal to the nozzle face and the green beams producing fringe patterns parallel to the face and oriented to measure a vertical velocity. Hence, the blue beams always sensed the axial velocity component (U_z) while the green beams sensed either the radial velocity (U_r) or the tangential velocity (U_θ). The locations of the measurement volumes and the fringe orientations established that a *positive radial velocity* was *toward the center*, and a positive tangential velocity was clockwise when viewed looking downstream (i.e., right-hand rule about the axial velocity vector). Data were acquired for circumferential traverses of the flow as achieved by rotating the nozzle in 5-deg increments for each of eight radial positions. Operation of the system was completely automated; approximately 30 s were required to acquire, process, and store data for 512-point PDFs on each of the two channels and to position the equipment to the next measurement station. A numerically controlled milling machine bed was used to position the velocimeter. The actuation of this bed was used to position the velocimeter. The actuation of this bed and the rotary table and the collection/storage of the velocimeter data were governed by an Apple IIe microcomputer equipped with 128K of random access memory (RAM). Reference marks were used to initialize the rotary table; a fine wire target, inserted into the nozzle precisely on its centerline, was used to zero the position of the velocimeter.

Test Results

The test program described above studied eight model aerating nozzle configurations in order to determine the airflow characteristics produced by them. The magnitude of data collected for the 12 measurement planes indicated in Table 1 is too great to fully discuss in a single publication. The focus

Table 1 Airflow data sets

	Configuration	Data plane, z (in.)	Data type
1	Baseline	0.060,2.50	U_z, U_r, U_θ, $\overline{u_z'}$, $\overline{u_r'}$, $\overline{u_\theta'}$, $\overline{u_z'u_\theta'}$, $\overline{u_z'u_r'}$
8	Misaligned endcap	0.060	U_z, U_r, U_θ, $\overline{u_z'}$, $\overline{u_r'}$, $\overline{u_\theta'}$
18	Reduced outer vanes	0.060, 2.50	U_z, U_r, U_θ, $\overline{u_z'}$, $\overline{u_r'}$, $\overline{u_\theta'}$
17	Reduced inner vanes	0.060, 2.50	U_z, U_r, U_θ, $\overline{u_z'}$, $\overline{u_r'}$, $\overline{u_\theta'}$
23	Extended core baseline	0.060, 2.50	U_z, U_r, U_θ, $\overline{u_z'}$, $\overline{u_r'}$, $\overline{u_\theta'}$, $\overline{u_z'u_\theta'}$, $\overline{u_z'u_r'}$
31	Tandem inner swirler	0.060	U_z, U_r, U_θ, $\overline{u_z'}$, $\overline{u_r'}$, $\overline{u_\theta'}$, $\overline{u_z'u_\theta'}$, $\overline{u_z'u_r'}$
19	Square-edge outer swirler	0.060	U_z, U_r, U_θ, $\overline{u_z'}$, $\overline{u_r'}$, $\overline{u_\theta'}$, $\overline{u_z'u_\theta'}$, $\overline{u_z'u_r'}$
20	Knife-edge outer swirler	0.060	U_z, U_r, U_θ, $\overline{u_z'}$, $\overline{u_r'}$, $\overline{u_\theta'}$, $\overline{u_z'u_\theta'}$, $\overline{u_z'u_r'}$

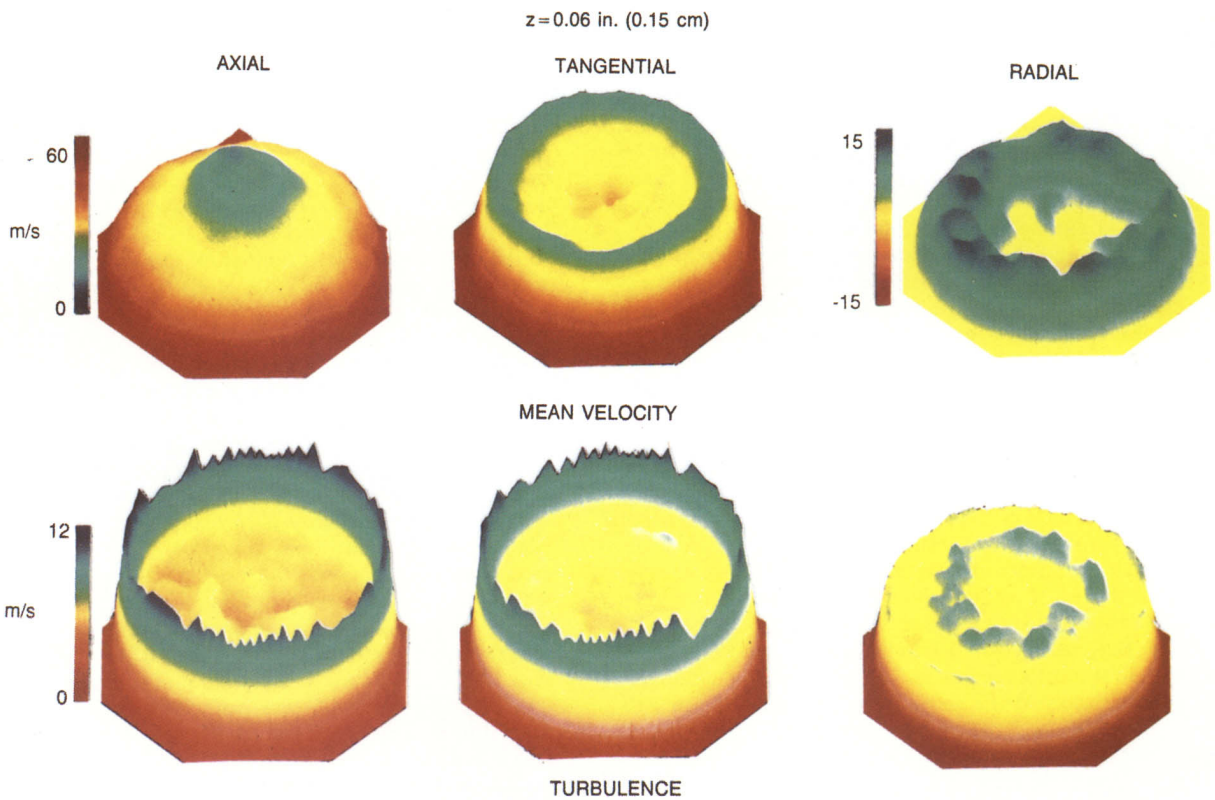

Fig. 3 Isometric velocity and turbulence contours for baseline.

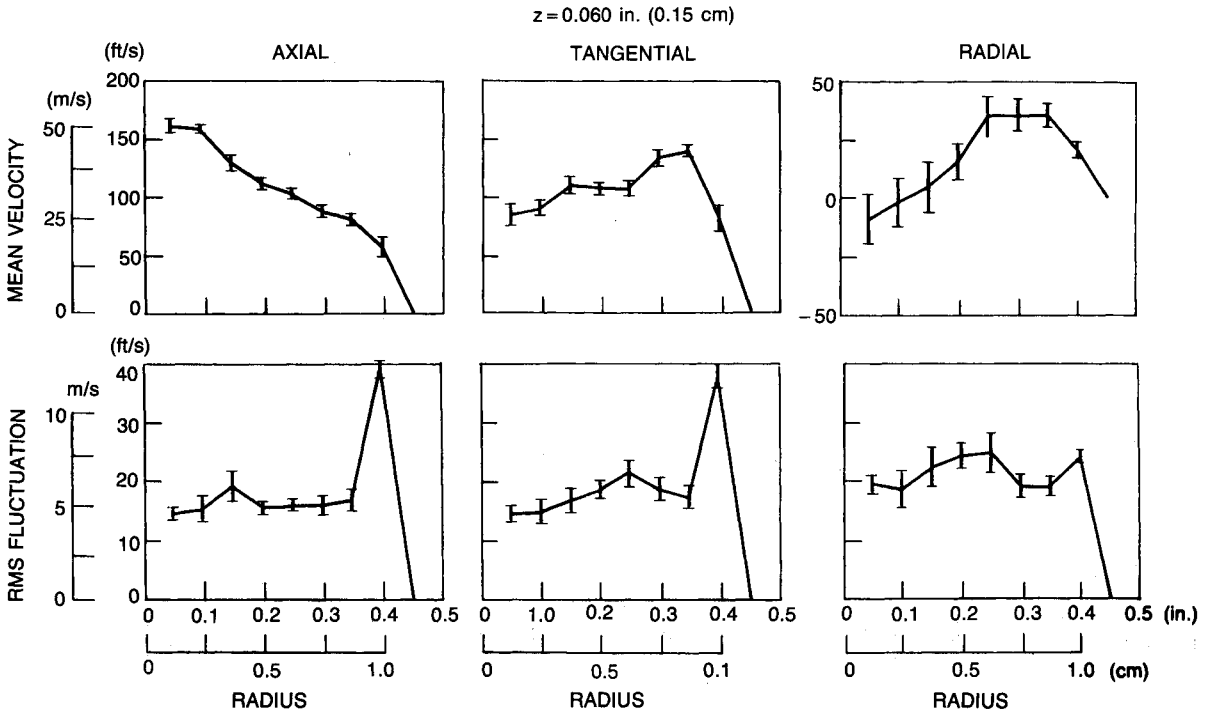

Fig. 4 Mean radial profiles of velocity and turbulence for baseline.

here will be to describe many features of the airflow established by the baseline configuration and then to describe how the subsequent nozzle configurations altered it.

Baseline Configuration Airflow

The airflow patterns 0.060 in. (1.5 mm) downstream from the baseline configuration are represented by the isometric contour plots depicted in Fig. 3. The first row depicts the mean axial, tangential, and radial velocities; the second row presents the corresponding normal turbulent velocities. Although only qualitative, these profiles convey an important sense of the complex flow exiting this nozzle. All of the profiles were nearly axisymmetric as expected, with regions of high turbulence generation occurring in the outer shear layers. These and other features are quantified by the plots contained in Fig. 4, which display the circumferentially averaged values for the velocity and turbulence measurements at each radial station. The "error bars" indicate a one standard deviation limit of the 72 data averaged at each radius.

These average radial profiles demonstrate the high degree of axisymmetry achieved and indicate the magnitude of the measured quantities. The axial velocity was center peaked and therefore gave no indication that the swirl generated by this nozzle produced a center recirculation zone. Axial velocities approaching 170 ft/s (53 m/s) were in agreement with the airflow pressure loss for these ambient temperature tests. Integration of the axial velocity over the nozzle area determined the air mass flow distribution and hence provided another indicator of flow uniformity. Following the practice for fuel spray distribution, the airflow uniformity was in fact much better than observed for the spray results for this configuration (depicted in Fig. 2a). Since the velocity measurements indicated that a high degree of airflow control was achieved, the spray pattern variations must have resulted from fuel path effects.

Positive tangential velocities indicated the expected clockwise swirl. In the outer regions of the flow, the tangential velocities greatly exceeded the axial velocities with the opposite relation near the center. Together the axial and tangential velocities were used to calculate local swirl angles and a swirl number for the flow. The radial variation of swirl angle for the baseline is depicted in Fig. 5. The depicted swirl angle was calculated from a horizontal traverse across the nozzle at a

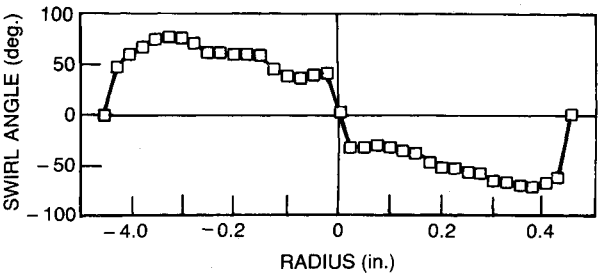

Fig. 5 Baseline exit swirl angle variation was regular.

downstream distance of 0.060 in. (1.5 mm). Because of the geometry and velocity relationships, the clockwise swirl was discerned as a positive swirl angle along the negative x axis and as a negative swirl angle along the positive x axis; in fact, the entire flow was swirling clockwise. The calculated angle was near to the measured vane turning angle (50 deg) for the outer regions decaying to much lesser levels near the core. The swirl number, often used as an indicator of vortex breakdown in the flow, is the ratio of the angular momentum and the product of the axial thrust and a characteristic radius. The swirl number calculated for this configuration was based on the ratio of angular momentum to axial momentum; no account was made of the pressure thrust. Based upon the radius at which the axial velocity dropped to zero, the swirl number was 0.62. There are various definitions and approximations to the swirl number[11]; for most cases a vortex breakdown and resulting central recirculation zone would be expected for this calculated swirl number. Such a separation was not evident, which indicates that such a single parameter did not sufficiently characterize these complex swirling flows. It was noted that the swirl number for the outer and inner swirlers alone, based upon the simple straight vane formulation, were 1 and 0.8, respectively. Each was notably larger than calculated from the velocity profiles; each represents a strong swirl, which would promote the vortex breakdown. Possibly the interaction of the two streams (as forced by the nozzle endcap) produced a flowfield poorly represented by a single swirl number.

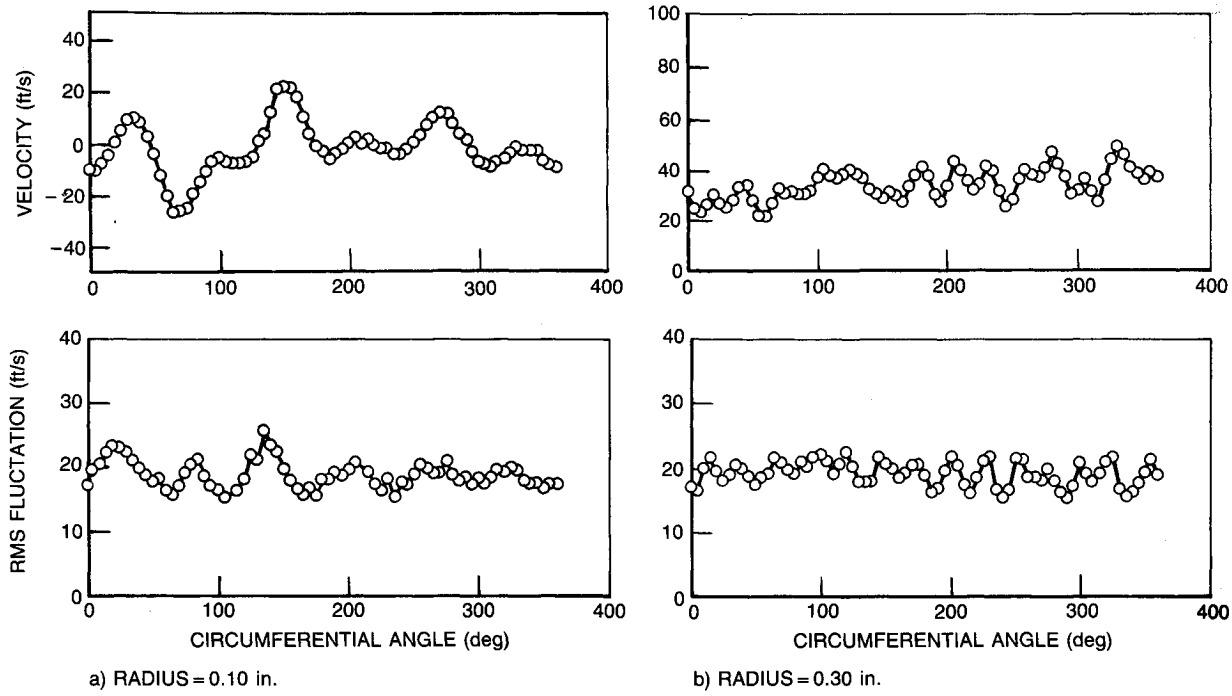

Fig. 6 Exit radial velocity and turbulence signatures for baseline.

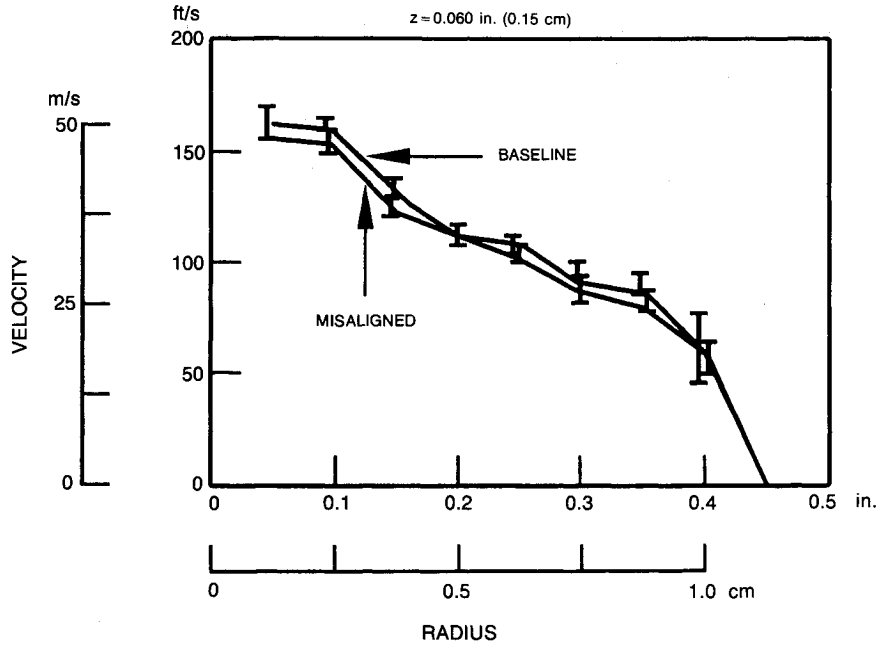

Fig. 7 Misaligned endcap delivered a symmetrical airflow.

Positive radial velocities indicated flow directed toward the centerline of the nozzle. The radial velocities (Figs. 3 and 4) were much lower than the others and registered a greater variation in magnitude (i.e., greater standard deviation), especially near the center regions of the flow. The root mean square (RMS) fluctuations of the radial velocity were nearly equal to, or exceeded, the mean radial velocity. These radial velocity data show that near the nozzle face, flow from the outer swirler was directed inward while the core-swirler air moved outward; the zero radial velocity region was near the radius of the annular fuel gap. It was likely that the interaction of these streams contributed to the radial velocity variations, a flow situation that ought to aid fuel atomization. It appeared that the wakes from the swirler vanes also contributed to the flow variations. Figure 6 depicts the measured radial velocity and turbulence data around the nozzle at radial positions of 0.1 in. (2.5 mm) and 0.3 in. (7.6 mm); the former is within the core flow and the latter is in the outer swirling stream. Although of differing magnitude, periodic variations of the radial velocity and fluctuation were observed, with six local peaks evident for the inner flow and 14 in the outer flow in direct correspondence to the number of swirler vanes; harmonic analyses also identified these as dominant modes. The magnitude of these variations was greater for the inner flow, consistent with the greater deviations and turbulence indicated above. These observations were also consistent with the fuel spray results, which indicated that variations on the inner swirler had a greater impact on patternation than variations on the outer swirler. It was argued that inner swirler variations were effectively more intense because they were confined to a smaller flow area. These velocity data confirm that potentially similar wake disturbances had a greater influence on the inner flow.

Except for the outer shear region, the turbulence appeared isotropic with each RMS fluctuation approximately 20 ft/s (6 m/s). The turbulence intensity was 16 to 20% of the local, total velocity vector magnitude over the bulk of the flow with a 60% intensity registered in the outer shear region. This increase was due to a near doubling of the fluctuation magnitude and a 40% reduction of the total velocity magnitude.

Altered Configurations

The misaligned aircap configuration inclined the outer swirler and endcap by 2.5 deg from true axial. As described, however, the nozzle was mounted to a rotary table by a flange attached to the endcap. Therefore, as mounted, the endcap was axially aligned and the inner components of the nozzle deviated by 2.5 deg. The velocity profiles 0.060 in. (1.5 mm) downstream from the nozzle were axisymmetric. Figure 7 displays the mean radial profiles for axial velocity for this configuration and the baseline. The standard deviation in the core region averaged 2.6 ft/s (0.8 m/s) for the misaligned configuration and 4.8 ft/s (1.5 m/s) for the baseline. Clearly the presence of the 2.5-deg misaligned core swirler flow was not sensed; the bulk airflow was dominated by the outer flow. The fuel spray pattern produced by this configuration was not axisymmetric, however (Fig. 2b). The pattern was shifted approximately 0.18 in. (4.6 mm) off center representing a 4-deg steering. More importantly, the pattern was not only shifted but also skewed to result in a very nonuniform fuel mass flux. Three regions of higher fuel mass flux were discerned in the fuel patternation. Therefore, an altered interaction of the air and fuel streams at the filming lip was probably a stronger influence on the resulting pattern than the alignment. Detailed studies within the nozzle would be necessary to document this effect.

Two configurations were studied to determine the influence of reducing the number of vanes in either the inner or outer swirler. The fuel spray formed by the outer swirler configuration of the reduced vanes displayed seven regions of high fuel mass flux in direct correspondence to the number of swirler vanes. Similarly, seven distinct regions of high air flux were also evident. This was particularly true for the radial velocities where strong cyclic variations between inward and outbound flow were sensed. This latter feature is more clearly presented in traverses for radial velocity and fluctuation obtained at radial positions of 0.15 and 0.35 in. (3.8 and 8.9 mm) (Fig. 8). The seven distinct cycles discerned for both radii indicated the spread of the influence over the entire flow. The velocity variations imposed by the removal of alternate outer swirler vanes (equivalently, increasing the gap-to-cord ratio in the swirler) were most prominent for the radial velocity because it had the lowest magnitude. Periodic variations in both the axial and tangential velocities were also present. Analyses of these velocity components suggested that the fuel mass flux variations correspond to the regions of increased axial velocity. The patternation data were fuel mass flux and not fuel concentration values; regions of high airflow velocity convected higher flow rates of fuel. At the radius of maximum variation, 55% of the fuel flow radius, the total velocity ranged from 167 to 138 ft/s (51 to 42 m/s) or a maximum to minimum ratio of 1.2. The full patternation of this configuration contained maximum fuel flux variations at 50% of the fuel spray radius, with a ratio of the maximum to minimum mass flux of approximately 1.7. Therefore, while regions of high axial flow likely did convect higher local fuel flow rates, a fuel-air interaction in the nozzle must have occurred to further enhance this effect. It is important to note that these influences were imposed in the vicinity of the nozzle exit but were not apparent in the velocity distributions further downstream from the nozzle. Figure 9 depicts air velocity and fuel flux contours at both the nozzle exit and further downstream. Although apparent at the nozzle exit, regular velocity variations resulting from the number of swirl vanes could not be discerned in data recorded 2.5 in. (6.4 cm) downstream. Hence, while the airflow signature decayed, its influence on the fuel flux leaving the nozzle persisted. The flow characteristics observed for the configuration with the reduced number of core swirler vanes were similar to those described for the outer swirler variation. That is, the use of a three-vane swirler resulting from removal of alternate vanes from the core swirler produced a flowfield that reflected the three vanes.

Two configurations used outer swirlers with each trailing edge altered to produce either a sharp (knife) edge or a blunt (square) edge; the baseline configuration had rounded trailing edges. Velocity data were acquired only 0.060 in. (1.5 mm) downstream of the nozzle in an attempt to sense a significant difference in the turbulence levels produced by these configurations. Fuel patternation data acquired previously indicated that only small differences were produced from the use of these differing trailing edges. Figure 10 displays mean radial

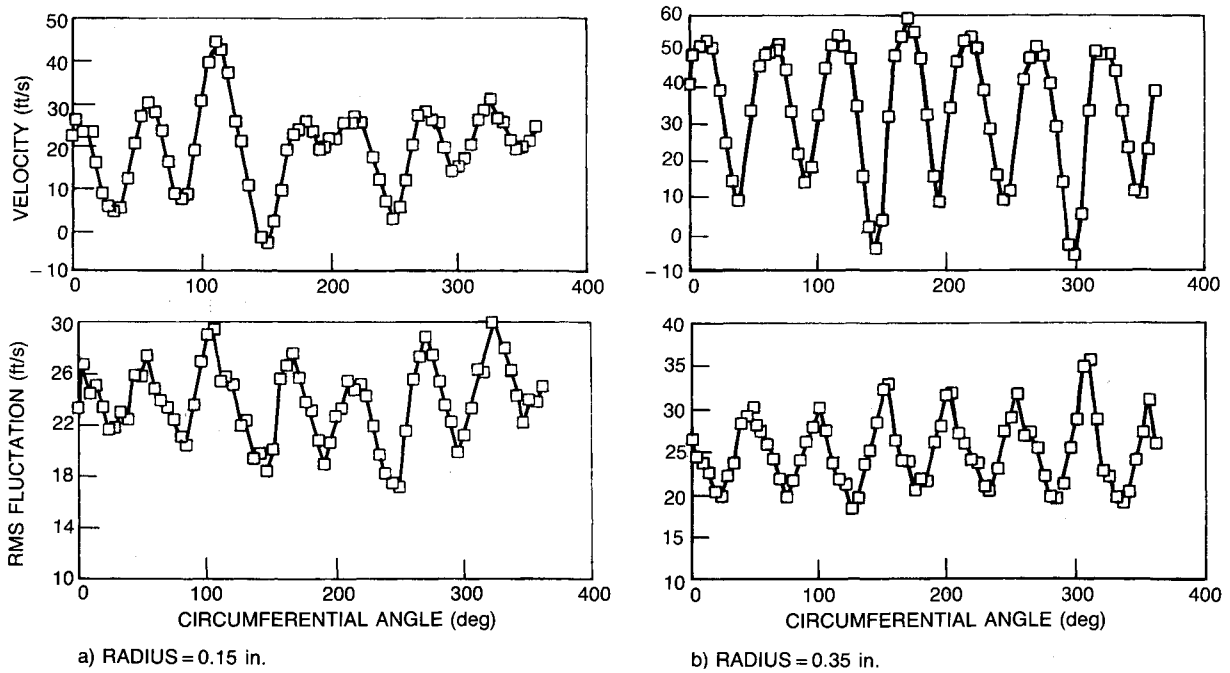

Fig. 8 Exit radial velocity and turbulence signatures reflected removal of swirler vanes.

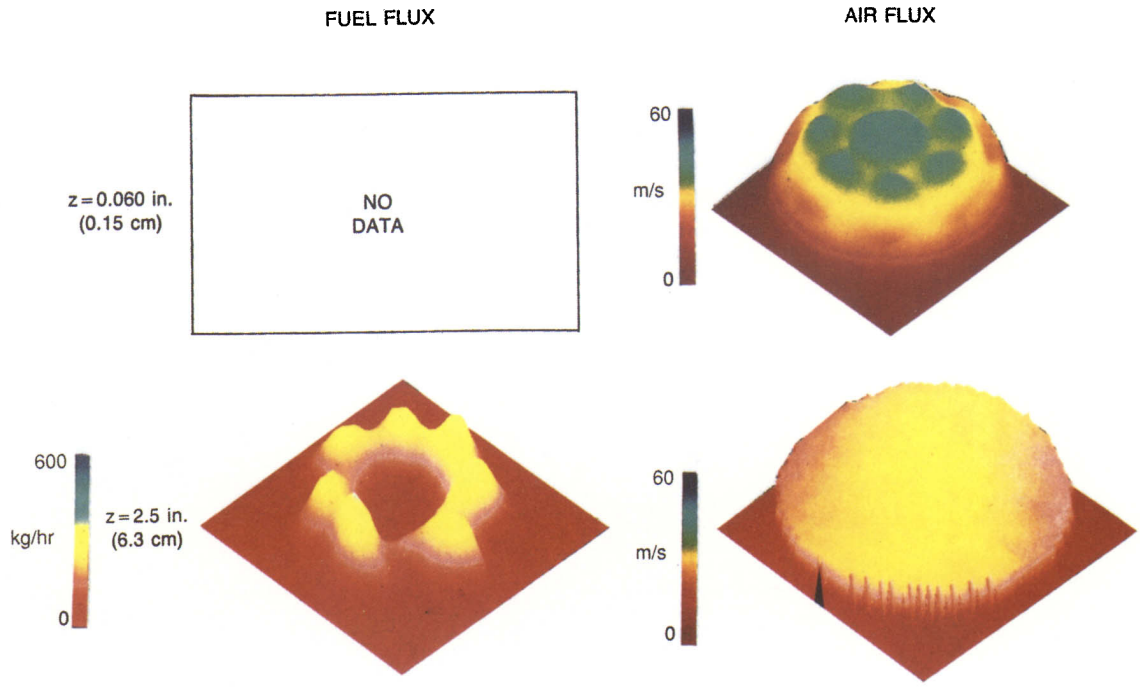

Fig. 9 Persistence of fuel and air distributions.

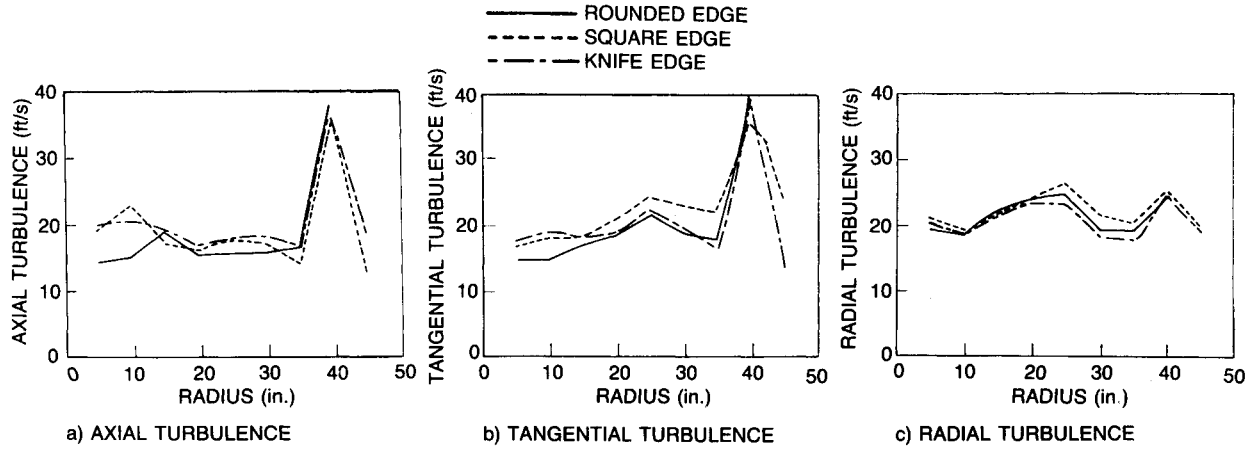

Fig. 10 Turbulence profiles were independent of swirler trailing edge shape.

profiles for the axial, tangential, and radial turbulence levels for these three configurations. No regular influence was discerned; no particular trailing edge shape appeared to generate greater or lesser turbulence levels. Therefore, there appears to be no need (from a fuel circumferential patternation point of view) to achieve highly streamlined trailing edges on conventional swirlers.

A nozzle configuration was assembled that included two six-vane core swirlers in tandem. For this configuration, the core air pipe was extended upstream to accept the two swirlers; the velocity and turbulence characteristics of this altered baseline (i.e., extended-core baseline) were essentially the same as the original baseline configuration. The two core swirlers were mounted to place the trailing edge of the upstream vanes in the center of the gap at the inlet plane to the downstream swirler. That is, the swirlers were oriented to place the wake regions from the upstream swirlers in the inlet flow to the downstream swirler. The purpose of this configuration was to determine if these upstream disturbances could be discerned in the velocity and turbulence characteristics at the nozzle exit. A comparison of the contour plots and the mean radial profiles for these quantities contained no components produced by the upstream most swirler. As for the baseline configuration, the presence of flow disturbances was most easily detected by examining the traverses for radial velocity and turbulence (Fig. 11) at radial positions of 0.1 and 0.3 in. (2.5 and 7.6 mm). Fourteen cycles of the radial velocity and turbulence can be observed at the outer radius in response to the 14 vanes in the outer swirler. Less than six cycles are observed for radial velocities at 0.1 in. (2.5 mm), a trend similar to that observed for the baseline configuration (Fig. 6a); harmonic analyses revealed no organized variation near 12 Hz. This result suggests that the swirler itself is the dominant influence on the velocity and turbulent fields downstream of it; turbulent disturbances occurring upstream of the swirler appeared not to be transmitted through it. Similarly, it would be expected that reasonable variations in the turbulence levels upstream of the fuel nozzle would not significantly alter the fuel atomization and distribution process. Of course, extreme deviations as might be experienced during compressor stall or surge would clearly be transmitted through the swirler and strongly influence the fuel pattern.

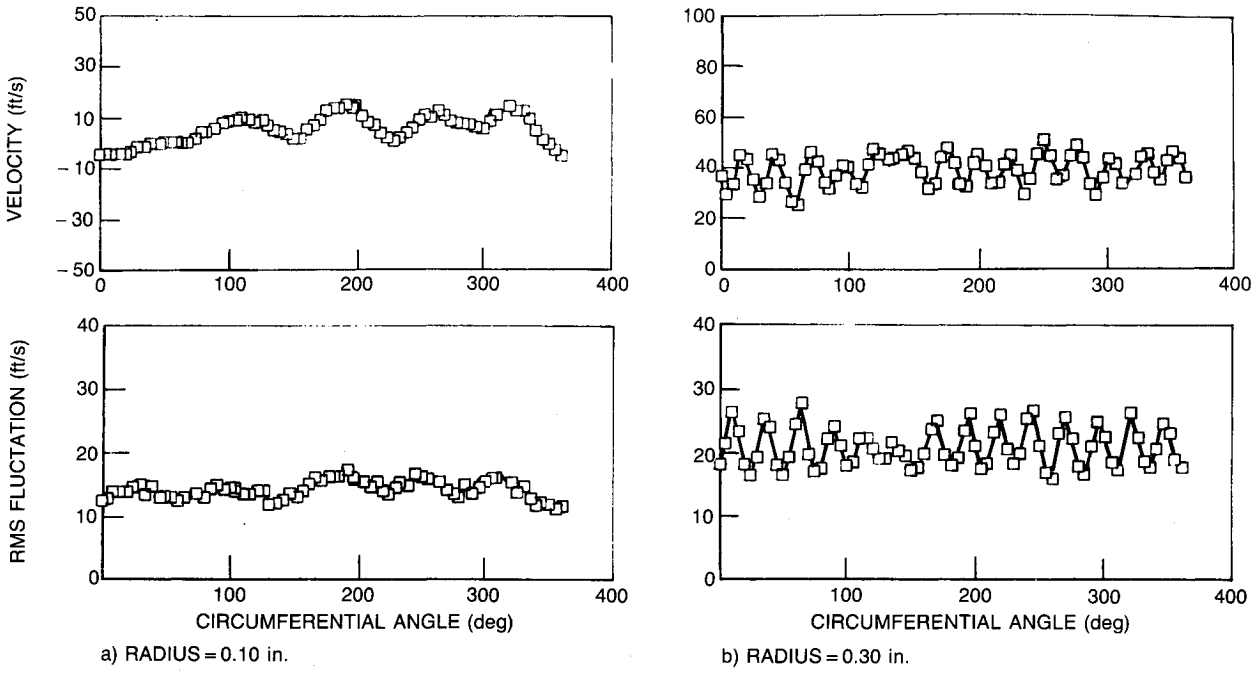

Fig. 11 Exit radial velocity and turbulence signatures did not reflect upstream disturbances.

Discussion and Conclusion

Detailed measurements of the airflow and turbulence have been made downstream of several configurations of a model aerating fuel nozzle. The nozzle assemblies included a symmetric baseline and others that purposefully altered the airflow by misaligning swirlers, changing the number of vanes in a swirler, or contouring the vane trailing edge. These data sets may be useful in evaluating the effectiveness of computational codes at predicting the evolution of multidimensional, swirling airflows.

The velocity and turbulence data that document the airflow profiles at the nozzle exit and further downstream directly support the following conclusions:

1) Highly axisymmetrical mean velocity profiles can be produced by an aerating fuel nozzle.

2) Significant variations in the airflow profile at the nozzle exit mix out rapidly to produce a uniform profile within three exit diameters downstream of the nozzle.

3) The flow in the swirler passages dominate in establishing the velocity and turbulence field downstream of the nozzle. Upstream disturbances are not easily transmitted through it; practical changes of the swirler trailing edge condition are on a smaller scale than the passage scale, which result in only minor alterations to the velocity and turbulence fields.

These conclusions can be integrated with those regarding nozzle design influences on fuel sprays to observe the following:

1) Since the airflow profiles were very axisymmetrical, whereas the spray patterns were notably less axisymmetrical despite attempts to achieve a uniform fuel gap, the nozzle patternation quality must be highly dependent on the fuel distribution in the nozzle.

2) Nozzle assemblies that purposefully perturbed the airflow were evaluated. The airflow profiles responded directly to the perturbation, and the effect on the fuel spray pattern was greater than the perturbation. It is concluded that air-fuel interactions within the nozzle are important processes that influence the resulting spray patternation. Substantial fuel nonuniformities that persist for considerable downstream distances can be produced.

3) The capacity of the airflow swirlers to filter out upstream disturbances from significantly affecting downstream flowfields indicates that spray atomization and distribution results will also be insensitive to such upstream disturbances.

Acknowledgments

This study was performed at UTRC under the sponsorship of the U.S. Air Force Aero-Propulsion Laboratory, Wright-Patterson Air Force Base, Ohio (Contract F33615-85C-2515); the Program Managers were Ruth Sikorsky and Royce Bradley. The continuing support of UTRC studies and capabilities by United Technologies Corporation (UTC)/Pratt & Whitney is also appreciated.

References

[1]Kilik, E., "The Influence of Swirler Design Parameters on the Aerodynamic Characteristics of the Downstream Recirculation Region," Ph.D. Thesis, Cranfield Institute of Technology, Cranfield, England, UK, May 1976.

[2]Kilik, E., "Better Swirl Generation by Using Curved Vane Swirlers," AIAA Paper 85-0187, Jan. 1985.

[3]Kilik, E., "Influence of the Blockage Ratio on the Efficiency of Swirl Generation with Vane Swirlers," AIAA Paper 85-1103, July 1985.

[4]Sander, G. F., and Lilley, D. G., "The Performance of an Annular Vane Swirler," AIAA Paper 83-1326, Jan. 1983.

[5]Lilley, D. G., "Swirling Flows in Typical Combustor Geometries," AIAA Paper 85-0184, Jan. 1985.

[6]Martin, C. A., "Aspects of the Design of Swirlers as Used in Fuel Injectors for Gas Turbine Combustors," American Society of Mechanical Engineers Paper 87-GT-139, June 1987.

[7]Martin, C. A., "Air Flow Performance of Air Swirlers for Gas Turbine Fuel Nozzles," American Society of Mechanical Engineers Paper 88-GT-108, June 1988.

[8]Smith, C. E., et al., "Fuel Injector Characterization and Design Methodology to Improve Lean Stability," AIAA Paper 85-1183, July 1985.

[9]Rosfjord, T. J., and Russell, S., "Influences on Fuel Spray Circumferential Uniformity," AIAA Paper 87-2135, June 1987; see also *Journal of Propulsion and Power*, Vol. 5, No. 2, 1989, pp. 144–150.

[10]McVey, J. B., Kennedy, J. B., and Russell, S., "Application of Advanced Diagnostics to Airblast Injector Flows," American Society of Mechanical Engineers Paper 88-GT-12, June 1988.

[11]Gupta, A. K., Lilly, D. G., and Syred, N., *Swirling Flows*, Abacus Press, 1984.